

Spin Orientation and Spin Precession in Inversion-Asymmetric Quasi Two-Dimensional Electron Systems

R. Winkler

Institut für Technische Physik III, Universität Erlangen-Nürnberg, Staudtstr. 7, D-91058 Erlangen, Germany
(dated: May 14, 2003)

Inversion asymmetry induced spin splitting of the electron states in quasi two-dimensional (2D) systems can be attributed to an effective magnetic field B which varies in magnitude and orientation as a function of the in-plane wave vector k_k . Using a realistic 8×8 Kane model that fully takes into account spin splitting because of both bulk inversion asymmetry and structure inversion asymmetry we investigate the spin orientation and the effective field B for different configurations of a quasi 2D electron system. It is shown that these quantities depend sensitively on the crystallographic direction in which the quasi 2D system was grown as well as on the magnitude and orientation of the in-plane wave vector k_k . These results are used to discuss how spin-polarized electrons can precess in the field $B(k_k)$. As a specific example we consider $Ga_{0.47}In_{0.53}As$ -InP quantum wells.

I. INTRODUCTION

Spin degeneracy in a two-dimensional (2D) system is due to the combined effect of spatial inversion symmetry and time inversion symmetry.¹ If the spatial inversion symmetry is lifted spin-orbit interaction gives rise to a spin splitting of the electron states even at a magnetic field $B = 0$. In quasi 2D systems the $B = 0$ spin splitting can be caused by the bulk inversion asymmetry (BIA) of the underlying crystal structure² as well as by the structure inversion asymmetry (SIA) due to, e.g., an electric field E perpendicular to the plane of the 2D system.³ The $B = 0$ spin splitting is of considerable interest both because of its importance for our understanding of the fundamental properties of quasi 2D systems^{4,5,6,7} as well as because of possible applications in the field of spintronics.⁸

Common III-V and II-VI semiconductors such as GaAs, InSb, and HgCdTe, have a zinc blende structure. To lowest order in the wave vector k BIA spin splitting in these systems is characterized by the so-called Dresselhaus term² whereas spin splitting due to SIA is characterized by the Rashba term.³ Often the discussion of spin splitting is restricted to these lowest-order terms.^{9,10,11,12} Spin splitting of higher orders in k can be fully taken into account by the 8×8 Kane model¹³ or the 14×14 extended Kane model.¹⁴ The higher-order terms can be quite important for a quantitative discussion of $B = 0$ spin splitting.^{15,16}

For a given in-plane wave vector k_k we can always find a spin axis $h_s(k_k)$ local in k_k space such that we have spin-up and spin-down eigenstates with respect to the axis $h_s(k_k)$. Note that we cannot call the spin-split branches $E_{\uparrow}(k_k)$ of the energy surface spin-up or spin-down because the direction of h_s varies as a function of k_k such that averaged over all occupied states the branches contain equal contributions of up and down spin components. This reflects the fact that in nonmagnetic materials we have at $B = 0$ a vanishing magnetic moment.

The spin orientation $h_s(k_k)$ can be attributed to an

effective magnetic field $B(k_k)$ (Refs. 9,17). A discussion of $h_s(k_k)$ based on the lowest-order terms in the effective spin-orbit interaction has previously been given by several authors, see, e.g., Refs. 18,19,20,21,22. In the present paper we compare these results with our calculations of $h_s(k_k)$ and the field $B(k_k)$ using the more realistic 8×8 Kane model¹³ that takes into account both SIA and BIA up to all orders in k_k . It will be shown that for larger k_k the higher-order terms result in important modifications of $h_s(k_k)$ and $B(k_k)$.

Datta and Das have proposed a novel spin transistor¹⁸ where the current modulation arises from the precession of spin-polarized electrons in the effective field $B(k_k)$, while ferromagnetic contacts are used to preferentially inject and detect specific spin orientations. Recently, extensive research aiming at the realization of such a device has been under way.²³ Here we will use our results for the field $B(k_k)$ in order to discuss spin precession and its tunability for different device configurations. It will be shown that for certain configurations the precession of spin-polarized electrons is determined only by the tunable SIA spin splitting; but it is essentially independent of the magnitude of BIA spin splitting. For other configurations the tunability of spin precession is significantly suppressed due to the interplay of SIA and BIA.

We would like to emphasize that the present results apply only to electrons with an (effective) spin $j = 1/2$. Holes in the topmost valence band, on the other hand, have an effective spin $j = 3/2$ (Ref. 24). Therefore, spin orientation and spin precession in quasi 2D hole systems is qualitatively different from spin orientation and spin precession in quasi 2D electron systems. Hole systems will thus be covered in a future publication.

II. SPIN ORIENTATION OF 2D ELECTRON STATES

In the following we want to discuss the wave vector dependent spin orientation $h_s(k_k)$ for different models of spin splitting. We will compare the analytical results for

the Rashba model and Dresselhaus model with our more realistic calculations based on the 8 × 8 Kane Hamiltonian that takes into account SIA and BIA spin splitting up to all orders in k_k .

A. General Discussion

First we want to discuss the spin orientation in the presence of SIA. Here to lowest order in the in-plane wave vector $k_k = (k_x, k_y, 0)$ the spin splitting is characterized by the Rashba Hamiltonian³

$$H_{\text{SIA}} = (\alpha_x k_y - \alpha_y k_x) \sigma_z; \quad (1)$$

where α_x and α_y are Pauli spin matrices and α is a prefactor that depends on the constituting materials and on the geometry of the quasi 2D system. If we use polar coordinates for the in-plane wave vector, $k_k = k_k (\cos \theta; \sin \theta; 0)$, the spin splitting is given by

$$E^{\text{SIA}}(k_k) = \alpha k_k \quad (2)$$

independent of the angle θ and the eigenstates are

$$|j^{\text{SIA}}(k_k)\rangle = \frac{e^{ik_k r_k}}{2} \begin{pmatrix} 1 \\ \frac{1}{i e^{i\theta}} \end{pmatrix} \quad (3)$$

with $r_k = (x; y; 0)$ and envelope functions $\chi_k(z)$. In Eq. (3) we have assumed that the Rashba coefficient is positive. The spin orientation of the eigenstates (3) is given by the expectation value with respect to the vector of Pauli spin matrices.

$$\langle \sigma_x \rangle = \cos \theta, \quad \langle \sigma_y \rangle = \sin \theta, \quad \langle \sigma_z \rangle = 0 \quad (4a)$$

$$= \frac{1}{2} \begin{pmatrix} 1 & 0 \\ 0 & -1 \end{pmatrix} \begin{pmatrix} 1 \\ \frac{1}{i e^{i\theta}} \end{pmatrix} = \frac{1}{2} \begin{pmatrix} 1 & 0 \\ 0 & -1 \end{pmatrix} \begin{pmatrix} 1 \\ -i e^{-i\theta} \end{pmatrix} = \frac{1}{2} \begin{pmatrix} 1 & 0 \\ 0 & -1 \end{pmatrix} \begin{pmatrix} 1 \\ -i \cos \theta + \sin \theta \end{pmatrix} = \frac{1}{2} \begin{pmatrix} 1 & 0 \\ 0 & -1 \end{pmatrix} \begin{pmatrix} 1 \\ -i \cos \theta + \sin \theta \end{pmatrix} \quad (4b)$$

Note that Eq. (4) is independent of the envelope function $\chi_k(z)$ and the magnitude k_k of the in-plane wave vector. The spin orientation (4) of the eigenfunctions (3) as a function of the direction of the in-plane wave vector is indicated by arrows in Fig. 1 (a).

Next we want to discuss the spin orientation in the presence of BIA spin splitting. For quasi 2D systems in a quantum well (QW) grown in the crystallographic direction [001] the Dresselhaus term becomes^{10,11}

$$H_{\text{BIA}} = \beta_x k_x (k_y^2 - k_z^2) + \beta_y k_y (k_x^2 - k_z^2) \quad (5)$$

with a material-specific coefficient β . This equation can easily be diagonalized. We obtain a spin splitting

$$E^{\text{BIA}}(k_k) = \frac{1}{4} \sqrt{4\beta_x^2 k_x^2 + 4\beta_y^2 k_y^2 + 4\beta_z^2 k_z^2} \quad (6a)$$

$$= \frac{1}{4} \sqrt{4\beta_x^2 k_x^2 + 4\beta_y^2 k_y^2 + 4\beta_z^2 k_z^2} \quad (6b)$$

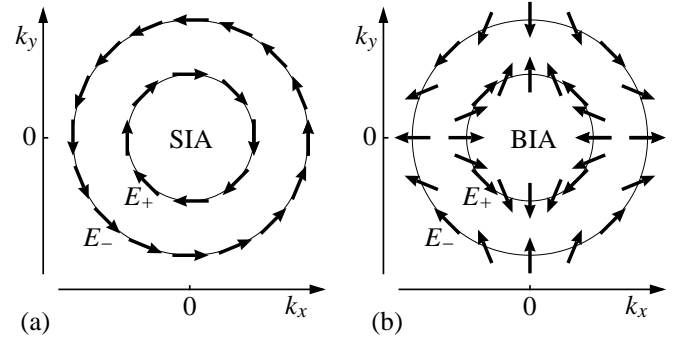


FIG. 1: Lowest order spin orientation $\langle \sigma \rangle$ of the eigenstates $|j(k_k)\rangle$ in the presence of (a) SIA and (b) BIA. The inner (outer) circle shows $\langle \sigma \rangle$ along contours of constant energy for the upper (lower) branch E_+ (E_-) of the spin-split dispersion.

We see here that in leading order of k_k the Dresselhaus term (5) gives rise to a spin splitting independent of the direction of k_k that is apparently very similar to the Rashba spin splitting (2). Nevertheless, the corresponding wave functions are qualitatively different due to the different symmetries of the terms (1) and (5). If we neglect the terms cubic in k_k the eigenfunctions in the presence of Dresselhaus spin splitting are

$$|j^{\text{BIA}}(k_k)\rangle = \frac{e^{ik_k r_k}}{2} \begin{pmatrix} 1 \\ \frac{1}{e^{i\theta}} \end{pmatrix} \quad (7)$$

so that

$$\langle \sigma_x \rangle = \cos \theta, \quad \langle \sigma_y \rangle = \sin \theta, \quad \langle \sigma_z \rangle = 0 \quad (8)$$

The spin orientation (8) of the eigenfunctions (7) as a function of the direction of the in-plane wave vector is indicated by arrows in Fig. 1 (b). For the Rashba spin splitting we see in Fig. 1 (a) that if we are moving clockwise on a contour of constant energy $E(k_k)$ the spin vector is rotating in the same direction, consistent with the axial symmetry of the Rashba term. On the other hand, Eq. (8) and Fig. 1 (b) show that in the presence of BIA the spin vector is rotating counterclockwise for a clockwise motion in k_k space.

In the above discussion we have assumed that the wave functions are two-component spinors. In general, the quasi 2D eigenstates of a multiband Hamiltonian are of the form²⁵

$$|j(k_k)\rangle = \frac{e^{ik_k r_k}}{2} \sum_n \chi_{nk_k}(z) u_n(r) \quad (9)$$

with envelope functions $\chi_{nk_k}(z)$, and $u_n(r)$ denotes the band edge Bloch function of the n th bulk band. Here we must evaluate the expectation value of

$$S = \frac{1}{2} \sigma_z; \quad (10)$$

where the identity operator $\mathbb{1}_{\text{orb}}$ refers to the orbital part of $j(k_k)i$. For the 8×8 Kane model¹³ containing the bands $\frac{c}{6}$, $\frac{v}{8}$, and $\frac{v}{7}$ we obtain for $i = x; y; z$

$$S_i = \begin{pmatrix} 0 & 1 \\ B & 0 \\ 0 & \frac{2}{3}J_i \\ 0 & 2U_i^y \end{pmatrix} \begin{pmatrix} 0 & 0 \\ 0 & 1 \\ \frac{2}{3}J_i & 2U_i^x \\ 2U_i^y & \frac{1}{3}i \end{pmatrix} \begin{pmatrix} 1 \\ 0 \\ 0 \\ 0 \end{pmatrix}; \quad (11)$$

where J_i denotes the matrices for angular momentum $j = 3/2$, and the matrices U_i are defined in Ref. 13. Once again the expectation value $\langle \mathbf{S} \rangle_j$ is a three-component vector that can be identified with the spin orientation of the multicomponent wave function $j i$. We remark that while the vector $\langle \mathbf{S} \rangle_i$ of a spin $l=2$ system is always strictly normalized to unity, this condition is in general not fulfilled for the spin expectation value $\langle \mathbf{S} \rangle_i$ of multicomponent single particle states. This is due to the fact that in the presence of spin-orbit interaction we cannot factorize the multicomponent wave function (9) into an orbital part and a spin part. However, for electrons the deviation of $\langle \mathbf{S} \rangle_i$ from unity is rather small (typically less than 1%) so that it is neglected here.

For free electrons in the presence of an external magnetic field B the unit vector \hat{h}_i is parallel to the vector B . Following this picture we can attribute the $B = 0$ spin splitting in quasi-2D system to an effective magnetic field $B(k_k)$ parallel to $\langle \mathbf{S} \rangle(k_k)i$. Obviously the magnitude of this effective magnetic field should be related to the magnitude of the $B = 0$ spin splitting. However, depending on the particular problem of interest it can be convenient to define the magnitude of spin splitting in two different ways: The energy difference $E = E_+(k_k) - E_-(k_k)$ characterizes the magnitude of spin splitting for a given wave vector k_k whereas the wave vector difference k characterizes the magnitude of spin splitting at a fixed energy E . While the former is relevant, e.g., for Raman experiments,¹⁵ the latter quantity is an important parameter, e.g., for spin relaxation^{6,17} and for the spin transistor proposed by Datta and Das.¹⁸

In the following we want to explore the second definition where the effective magnetic field is given by $B = \langle \mathbf{S} \rangle_i k$. Our precise definition of k is illustrated in Fig. 2: For the given energy E and a fixed direction \hat{k}' of the in-plane wave vector $k_k = k_k(\cos \hat{k}', \sin \hat{k}', 0)$ we determine $k_{k \parallel} = k=2$ such that $E = E_+(k_{k \parallel} = k=2) = E_-(k_{k \parallel} + k=2)$. Here E_+ (E_-) denotes the upper (lower) branch of the spin-split dispersion. Then we define

$$B = \langle \mathbf{S} \rangle_i k = \langle \mathbf{S} \rangle_i k_{k \parallel} \quad (12)$$

with the sign convention that the field B is parallel to the effective field felt by the electrons in the upper branch $E_+(k_k)$ and we have used the short-hand notation

$$\langle \mathbf{S} \rangle_i = \langle (k_k \parallel k=2) \mathbf{S} \rangle_i \quad (k_k \parallel k=2); \quad (13)$$

We remark that for a parabolic band with effective mass m plus Rashba term (1) the wave vector difference k

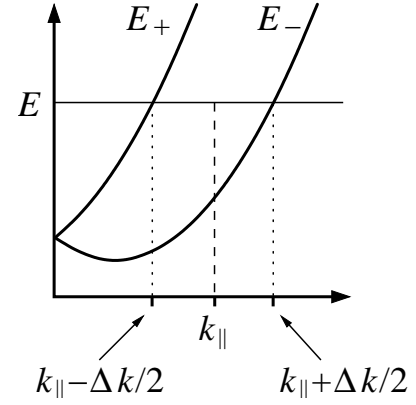


FIG. 2: For the given energy E and a fixed direction of the in-plane wave vector k_k we determine $k_{k \parallel} = k=2$ such that $E = E_+(k_{k \parallel} = k=2) = E_-(k_{k \parallel} + k=2)$. Here E_+ (E_-) denotes the upper (lower) branch of the spin-split dispersion.

can be evaluated analytically¹⁸

$$k_{\text{Rashba}} = \frac{2m}{\hbar^2} \quad (14)$$

independent of the magnitude of k_k . From an experimental point of view it should be kept in mind that spin splitting is often measured by analyzing Shubnikov-de Haas oscillations, see, e.g., Refs. 26,27,28,29. Such experiments yield spin subband densities N_{\pm} which are directly related to k

$$k = \frac{p}{4} \frac{p}{N_-} - \frac{p}{N_+}; \quad (15)$$

provided we can ignore anisotropic contributions to $B = 0$ spin splitting. (However, see also Refs. 30,31.)

The definition (12) presupposes that the spin expectation values $\langle \mathbf{S} \rangle_i$ and $\langle \mathbf{S} \rangle_{i+}$ are strictly antiparallel to each other. In Eq. (4) we saw that for the Rashba Hamiltonian this condition is fulfilled exactly. This is closely related to the fact that for the Rashba Hamiltonian the spin subband eigenstates $j_+^{\text{STA}}(k_k)i$ and $j_-^{\text{STA}}(k_k)i$ are orthogonal (independent of the magnitude of k_k and k_k^0 as long as the wave vectors k_k and k_k^0 are parallel to each other.³² In general, $j_+(k_k \parallel k=2)i$ and $j_-(k_k \parallel k=2)i$ are only approximately orthogonal so that $\langle \mathbf{S} \rangle_i$ and $\langle \mathbf{S} \rangle_{i+}$ are only approximately antiparallel. However, we find that the angle between the vectors $\langle \mathbf{S} \rangle_i$ and $\langle \mathbf{S} \rangle_{i+}$ is always very close to 180° with an error $\sim 1^\circ$ so that we neglect this point in the remaining discussion.

Even though we can evaluate the spin expectation value $\langle \mathbf{S} \rangle_i$ for each spin subband separately we do not attempt to define an effective magnetic field B for each spin subband. This is due to the fact that B is commonly used to discuss phenomena like spin relaxation^{6,17} and spin precession¹⁸ (see below) which cannot be analyzed for each spin subband individually.

The allowed directions of the effective magnetic field B can readily be deduced from the symmetry of the QW.

The spin-split states for a fixed wave vector k_k are orthogonal to each other, i.e., the spin vectors of these states are antiparallel. The spin orientation of eigenstates for different wave vectors in the star of k_k are connected by the symmetry operations of the system.³³ Accordingly, only those spin orientations of the spin-split eigenstates are permissible for which every symmetry operation maps orthogonal states onto orthogonal states. In a QW grown in the crystallographic direction [001] the effective field B is parallel to the plane of the quasi-2D system. Indeed, the field B due to SIA is always in the plane of the well. For growth directions other than [001], the effective field due to BIA has, however, also an out-of-plane component. In particular, a symmetric QW grown in the crystallographic direction [110] has the point group C_{2v} .³⁴ Here the BIA induced field $B(k_k)$ must be perpendicular to the plane of the QW (to all orders in k_k). This situation is remarkable because D'yakonov-Perel' spin relaxation is suppressed if the spins are oriented perpendicular to the 2D plane.^{35,36} Note also that in [110] grown QW's B vanishes for $k_k \parallel [001]$ because here the group of k_k is C_{2v} which has merely one irreducible double group representation, Γ_5 , which is two-dimensional.³⁷

B. Numerical Results

The analytically solvable models (1) and (5) allow one to study the qualitative trends of BIA and SIA spin splitting in quasi-2D systems. The largest spin splitting can be achieved in narrow-gap semiconductors where the subband dispersion is highly nonparabolic. Therefore, we present next numerically calculated results for $B(k_k)$ obtained by means of an accurate 8 × 8 Kane Hamiltonian ($\frac{\epsilon}{6}$, $\frac{\nu}{8}$, and $\frac{\nu}{7}$) including off-diagonal remote band contributions of second order in k (Refs. 13,16). First we analyze BIA spin splitting that is always present in zinc blende QW's. In Fig. 3(a) we show the effective field (12) along contours of constant energy for a symmetric GaAs QW grown in the crystallographic direction [001] with a well width of 100 Å. The dimensions of the arrows in Fig. 3 are proportional to $|B_j| = k$. We remark that typical Fermi wave vectors of quasi-2D systems are of the order of the in-plane wave vectors covered in Fig. 3.

For small in-plane wave vectors k_k the effective field in Fig. 3(a) is well described by Eq. (8). For larger wave vectors the effective field becomes strongly dependent on the

direction of k_k . In particular, we see that for $k_k \parallel [110]$ the effective field reverses its direction when we increase k_k . This reversal reflects the breakdown of the linear approximation in Eq. (6). For wider wells this breakdown occurs at even smaller wave vectors k_k , consistent with Eq. (6).

More specifically, Eq. (6) predicts for $k_k \parallel [110]$ a reversal of the direction of $B(k_k)$ when $k_k^2 = 2\hbar k_z^2 i$, independent of the material specific coefficient β . Note, however, that $\hbar k_z^2 i$ depends on the material specific band offset at the interfaces. For the system in Fig. 3(a) we find in good agreement with Eq. (6) that the reversal of $B(k_k)$ occurs for $k_k = \frac{2\hbar k_z^2 i}{0.029 \text{ Å}^{-1}}$. For comparison, we show in Fig. 3(b) the effective field $B(k_k)$ for a symmetric $\text{Ga}_{0.47}\text{In}_{0.53}\text{As}$ QW with the same well width 100 Å like in Fig. 3(a). Even though BIA spin splitting is smaller in $\text{Ga}_{0.47}\text{In}_{0.53}\text{As}$ than in GaAs, higher-order corrections are more important in $\text{Ga}_{0.47}\text{In}_{0.53}\text{As}$ due to the smaller fundamental gap of this material. Here we have $\hbar k_z^2 i = 3.6 \cdot 10^{-4} \text{ Å}^{-2}$ so that $\frac{2\hbar k_z^2 i}{0.027 \text{ Å}^{-1}}$. On the other hand, the reversal of the direction of $B(k_k)$ occurs for $k_k = 0.021 \text{ Å}^{-1}$. This illustrates the effect of higher orders in BIA spin splitting that were neglected in Eq. (5) but fully taken into account in the numerical calculations in Fig. 3. [Note that in Fig. 3(a) the effective field B has been amplified by a factor of 50 whereas in Fig. 3(b) it has been amplified by a factor of 100.]

$\text{Ga}_{0.47}\text{In}_{0.53}\text{As}$ QW's can have a significant Rashba spin splitting³⁸ so that these systems are of interest for realizing the spin transistor proposed by Dutta and Das.¹⁸ In Fig. 3(c) we show the effective field $B(k_k)$ for the same well like in Fig. 3(b) assuming that we have SIA spin splitting due to an electric field $E = 20 \text{ kV/cm}$, but all tetrahedral terms that give rise to BIA spin splitting were neglected. The numerical results are in good agreement with what one expects according to Eqs. (4) and (14). Figure 3(d) shows the effective field $B(k_k)$ for a $\text{Ga}_{0.47}\text{In}_{0.53}\text{As}$ QW when we have both BIA and SIA spin splitting. Due to the vectorial character of B we have regions in k_k space where the contributions of BIA and SIA are additive whereas in other regions the spin splitting decreases due to the interplay of BIA and SIA. This is consistent with the well-known fact that in the presence of both BIA and SIA the spin splitting is anisotropic even in the lowest order of k_k (Ref. 9). Using Eqs. (1) and (5) we obtain

$$E^{BIA + SIA} = \frac{r}{k_k^2 + k_k^2 - 2\hbar k_z^2 i \sin(2')} + \frac{h}{k_k^2 + \frac{1}{4}k_k^2 - \hbar k_z^2 i k_k^2 \sin(2')^2} \quad (16a)$$

$$p \frac{h}{k_k^2 - 2\hbar k_z^2 i \sin(2') + 2\hbar k_z^2 i^2} \propto (k_k^3): \quad (16b)$$

In Figs. 3(a-d) we have considered QW's grown in the

crystallographic direction [001] so that the effective field

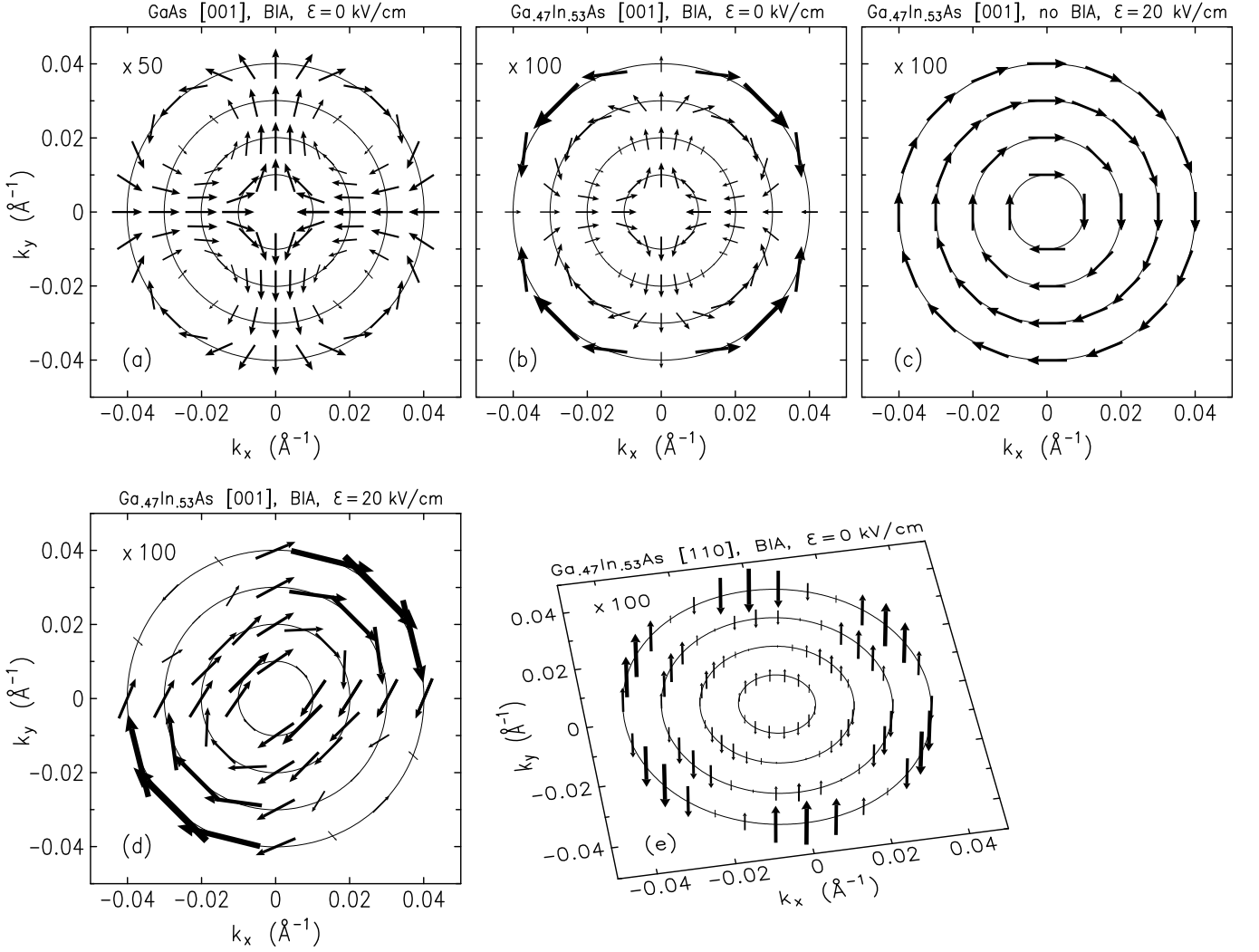


FIG. 3: Effective magnetic field $B(k_k)$ for (a) a GaAs- $\text{In}_{0.53}\text{Ga}_{0.47}\text{As}$ QW and (b-e) a $\text{Ga}_{0.47}\text{In}_{0.53}\text{As}$ -InP QW, both with a well width of 100 Å. In (a), (b), and (e) we assume that we have a symmetric well with BIA spin splitting only. (c) shows $B(k_k)$ due to an external field of $E = 20$ kV/cm but neglecting BIA while (d) shows $B(k_k)$ when we have both BIA and SIA spin splitting (again for $E = 20$ kV/cm). While (a-d) refers to a QW grown in the crystallographic direction [001] we have assumed in (e) that the QW was grown in [110] direction. The dimensions of the arrows are proportional to $|B| = \hbar k$. For $\text{Ga}_{0.47}\text{In}_{0.53}\text{As}$, we have amplified $B(k_k)$ by a factor of 100, for GaAs it has been scaled by a factor of 50. All calculations are based on an 8 × 8 Kane Hamiltonian ($\frac{c}{6}$, $\frac{c}{8}$, and $\frac{c}{7}$) including off-diagonal remote band contributions of second order in k (Ref. 13,16).

$B(k_k)$ is always in the plane of the QW. For comparison, we show in Fig. 3(e) the effective field $B(k_k)$ for a symmetric $\text{Ga}_{0.47}\text{In}_{0.53}\text{As}$ QW grown in the crystallographic direction [110] with $k_x \parallel [001]$ and $k_y \parallel [110]$. Here $B(k_k)$ is perpendicular to the plane of the QW.³⁵ For asymmetric QW's grown in the crystallographic direction [110] the effective field $B(k_k)$ is given by a superposition of an in-plane field as in Fig. 3(c) and a perpendicular field as in Fig. 3(e).

III. SPIN PRECESSION OF 2D ELECTRON STATES

A. Datta Spin Transistor

We want to briefly recapitulate the mode of operation of the spin transistor proposed by Datta and Das¹⁸ (see Fig. 4). We assume that the semiconducting channel between the ferromagnetic contacts is pointing in x direction, i.e., electrons travel with a wave vector $k_k = (k_x; 0; 0)$ from source to drain. A gate in z direction gives rise to a tunable Rashba coefficient. In this subsection we want to ignore the Dresselhaus spin splitting (5). When the spin-polarized electrons in the ferro-

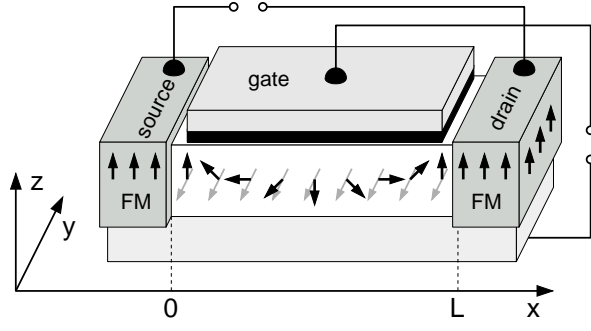


FIG. 4: Qualitative sketch of a Datta spin transistor.¹⁸ Black arrows indicate the spin polarization in the ferromagnetic contacts (FM) and the semiconducting channel (white). Gray arrows indicate the effective magnetic field $B(k_x)$ in the semiconducting channel. A top gate is used to tune the spin precession by applying an electric field E perpendicular to the semiconducting channel.

magnetic source contact are injected at $x = 0$ into the semiconducting channel we must expand its wave function j_i in terms of the spin-split eigenstates $j^{SIA}(k_x)$. Here it is the basic idea of the spin transistor that the polarization of the electrons in the source contact is chosen perpendicular to $B(k_x) = (0; B_y; 0)$. The states j_i thus contain equal contributions of the spin-split eigenstates $j^{SIA}(k_x)$. Assuming that the electrons in the source contact are polarized in $+z$ direction we get (neglecting the envelope functions $\psi_{k_x}(z)$ which are unimportant in the present discussion)

$$j_i(x=0) = \frac{1}{2} = \frac{1}{2} \left(\frac{1}{i} + \frac{1}{i} \right) : \quad (17a)$$

The basis states on the right hand side of Eq. (17a) propagate with wave vectors $k_x = k/2$ as depicted in Fig. 2

$$j_i(x) = \frac{1}{2} \exp[i(k_x - k/2)x] \frac{1}{i} + \exp[i(k_x + k/2)x] \frac{1}{i} : \quad (17b)$$

Due to the different phase velocities of the basis states in Eq. (17b) we thus get

$$\hbar s(x) = \begin{pmatrix} 0 & \sin(kx) \\ \sin(kx) & 0 \end{pmatrix} A : \quad (18)$$

This equation can be visualized by saying that the spin vector $\hbar s$ of the state $j_i(x)$ precesses around the effective field $B(k_x) = (0; B_y; 0)$ (see Fig. 4). Note, however, that conventional spin precession³⁹ takes place as a function of time whereas in Eq. (18) the spin precesses as a function of position x .

Finally the drain contact at $x = L$ is ferromagnetic, too, the electrons can exit the semiconducting channel

only if the spin orientation $\hbar s(x=L)$ of the electrons matches the polarization P_D of the drain contact,

$$\cos \theta = P_D \cdot \hbar s(x=L) ; \quad (19)$$

where θ denotes the angle between P_D and $\hbar s(x=L)$. A large positive value of $\cos \theta$ indicates that the electrons can easily exit the semiconducting channel whereas a large negative value indicates that the spin-polarized current is suppressed. Assuming that $P_{SD} \parallel [001]$ we obtain from Eq. (18)

$$\cos \theta = \cos(kL) : \quad (20)$$

A tunable device is achieved if the wave vector difference k is varied by changing the Rashba coefficient α , see Eq. (14) and Fig. 4.

In the above qualitative discussion we have ignored details such as the resistance mismatch at the interfaces^{40,41,42} which are important for the practical realization of such a device. But these aspects do not affect the spin precession inside the semiconducting channel which is the subject of the present investigation.

B. Precession in the presence of BIA and SIA

In the preceding subsection we have assumed that only the Rashba term (1) contributes to spin splitting. Here the effective magnetic field $B(k)$ that characterizes the spin orientation of the eigenstates (3) is always perpendicular to the direction k_k of propagation in the spin transistor. In general, we have both SIA and BIA spin splitting so that the effective field $B(k)$ is a more complicated function of k_k , see Fig. 3. An arbitrarily oriented effective field $B(k)$ can be characterized by polar angles θ and ϕ , i.e., $B = k[\sin \theta \cos \phi; \sin \theta \sin \phi; \cos \theta]$. The corresponding orthonormal eigenstates are

$$j^I = \begin{pmatrix} e^{i\phi/2} \cos(\theta/2) \\ e^{i\phi/2} \sin(\theta/2) \end{pmatrix} \quad (21a)$$

$$j^{\#} = \begin{pmatrix} e^{i\phi/2} \sin(\theta/2) \\ e^{i\phi/2} \cos(\theta/2) \end{pmatrix} : \quad (21b)$$

For any values of the angles θ and ϕ , the spin states (21) represent a basis of the spin $1/2$ space. Similar to Eq. (17a) we can thus expand the wave function j_i of the spin-polarized electrons in the ferromagnetic source contact in terms of the basis states (21)

$$j_i(x=0) = \cos u j^I + \sin u e^{iv} j^{\#} \quad (22a)$$

with angles u and v . Thus we get for the precessing electrons inside the channel

$$j_i(x) = \exp[i(k_x - k/2)x] \cos u j^I + \exp[i(k_x + k/2)x] \sin u e^{iv} j^{\#} : \quad (22b)$$

Then the overlap of the spin vector $\langle \mathbf{h}(\mathbf{x}) \rangle$ with the field \mathbf{B} is given by

$$\langle \mathbf{h}(\mathbf{x}) \rangle \cdot \mathbf{B} = k \cos(2u) \quad (23)$$

independent of the position \mathbf{x} inside the channel and independent of the phase e^{iv} . This equation shows that in generalization of Eq. (18) the spin is precessing on a cone around the effective field \mathbf{B} where the cone angle is $2u$. The precession amplitude $k \cos(2u)$ is the largest when $u = \pi/4$ so that in Eq. (22) we have equal contributions of the spin-split states \uparrow and \downarrow . This corresponds to the situation that the spin polarization $\mathbf{P}_S = \langle \mathbf{h}(\mathbf{x} = 0) \rangle$ in the ferromagnetic source contact is perpendicular to $\mathbf{B}(\mathbf{k}_k)$. Spin precession is suppressed for $u = 0$ and $u = \pi/2$ when the spin polarization \mathbf{P}_S in the ferromagnetic source contact is parallel to $\mathbf{B}(\mathbf{k}_k)$ so that only one spin state (21) contributes in Eq. (22).

We have seen in Fig. 3 that for a fixed wave vector \mathbf{k}_k the orientation of $\mathbf{B}(\mathbf{k}_k)$ can change when the Rashba spin-orbit interaction is tuned by means of an external gate. It follows that the basic operating principle of the Datta spin transistor remains valid for the more general eigenstates (21) provided the polarization \mathbf{P}_S of the ferromagnetic source contact is orthogonal to $\mathbf{B}(\mathbf{k}_k)$ for all values of the external "knob" that is used to tune the spin-orbit interaction. If the condition $\mathbf{P}_S \perp \mathbf{B}(\mathbf{k}_k)$ is not strictly fulfilled the tunability of the spin transistor is reduced. We note that these conclusions are valid also for the more general eigenstates (9).

C. Numerical Results

We present next numerically calculated results for the spin precession in a spin transistor obtained by means of an 8 × 8 Kane Hamiltonian^{13,16} that takes fully into account both BIA and SIA. According to Fig. 3 the effective fields $\mathbf{B}(\mathbf{k}_k)$ due to BIA and SIA in a [001]-grown QW are always parallel to each other for $\mathbf{k}_k \parallel [\bar{1}\bar{1}0]$ and $\mathbf{k}_k \parallel [110]$. On the other hand, for $\mathbf{k}_k \parallel [100]$ the fields are perpendicular to each other so that we want to focus on these two extreme cases. We will again consider a 100 Å wide $\text{Ga}_{0.47}\text{In}_{0.53}\text{As-InP}$ QW, and we assume that the distance between source and drain contact is $L = 5 \mu\text{m}$. For ease of notation we will use a suitably rotated coordinate system (Fig. 4) such that the electrons always propagate in x direction, i.e., $\mathbf{k}_k = (k_x; 0; 0)$. We assume that the Rashba spin-orbit coupling is tuned by applying an electric field E perpendicular to the plane of the quasi-2D system (Fig. 4).

In Fig. 5 we show the overlap $\cos \chi$ between the spin vector $\langle \mathbf{h}(\mathbf{x} = L) \rangle$ and the polarization \mathbf{P}_D of the drain contact as a function of electric field E . We consider different polarization states \mathbf{P}_S of the source contact and it is assumed that $\mathbf{P}_S \perp \mathbf{P}_D$. The results in Fig. 5 can readily be understood by means of Fig. 3. (i) If $\mathbf{k}_k \parallel [\bar{1}\bar{1}0]$ or $\mathbf{k}_k \parallel [110]$ BIA is of little importance because

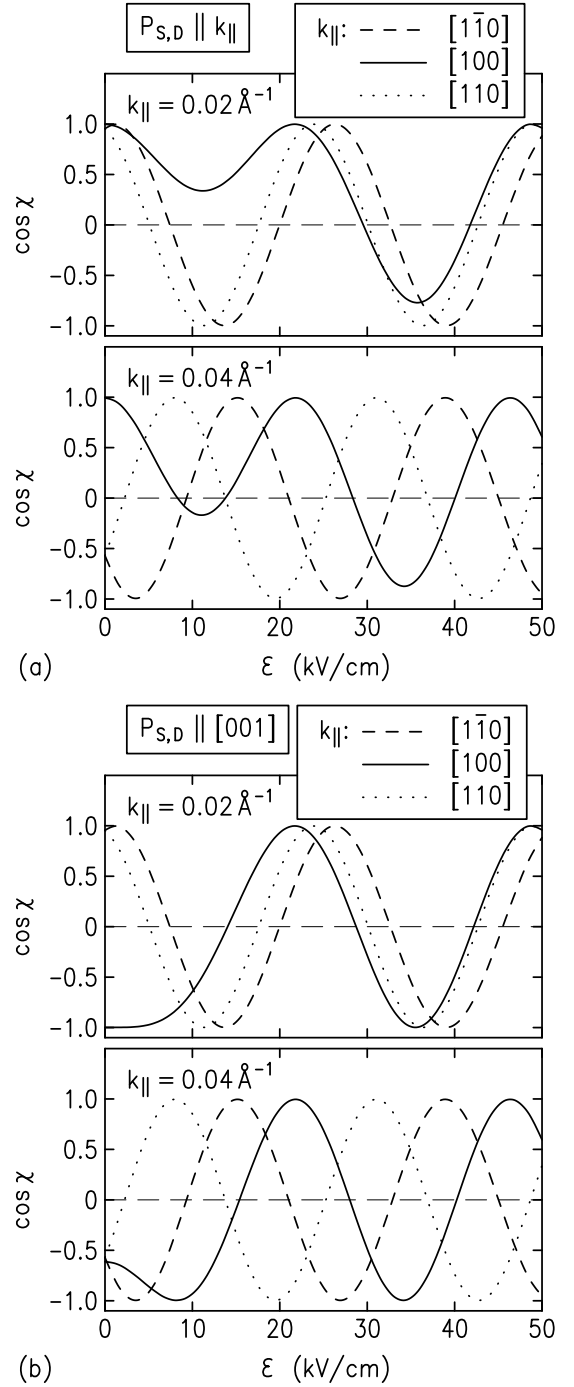


FIG. 5: Overlap $\cos \chi$ between the spin vector $\langle \mathbf{h}(\mathbf{x} = L) \rangle$ and the polarization \mathbf{P}_D of the drain contact as a function of electric field E in a 100 Å wide $\text{Ga}_{0.47}\text{In}_{0.53}\text{As-InP}$ QW with a channel length of $L = 5 \mu\text{m}$. In (a) we assume $\mathbf{P}_{S,D} \parallel \mathbf{k}_k$ whereas in (b) we assume $\mathbf{P}_{S,D} \parallel [001]$. Different line styles correspond to different crystallographic directions of \mathbf{k}_k as indicated. The calculations are based on an 8 × 8 Kane Hamiltonian ($\frac{c}{6}$, $\frac{v}{8}$, and $\frac{v}{7}$) including off-diagonal remote band contributions of second order in \mathbf{k} (Ref. 13,16).

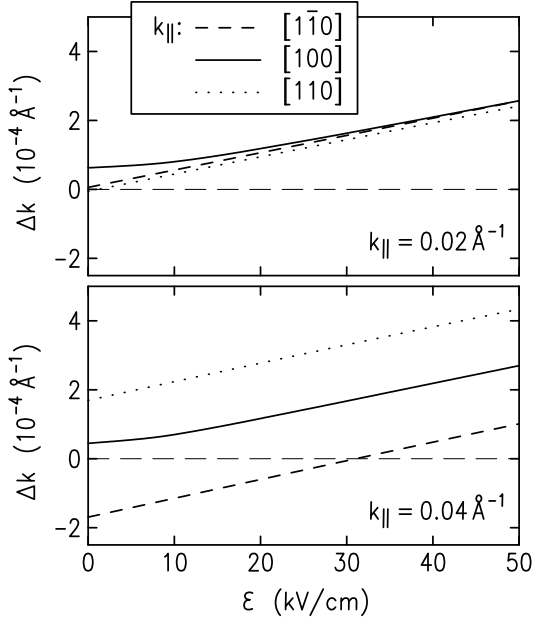


FIG. 6: Spin splitting k as a function of electric field E in a 100 Å wide $\text{Ga}_{0.47}\text{In}_{0.53}\text{As-InP}$ QW. We consider different magnitudes and different crystallographic directions of k_k as indicated in the figure.

$B_{\text{BIA}} k_{\text{BIA}}$. Consistent with Eq. (20) we thus get a sinusoidal dependence of \cos on E with the same angle for $P_{S,D} k_{\text{BIA}}$ and $P_{S,D} k_{\text{BIA}}$, see Figs. 5(a) and (b). We note that for fixed magnitudes of k_k and E the angle can be adjusted by changing the length L of the channel. In the present work L has not been optimized. Note that the smaller is the length L the larger must be the modulation of E for switching the device. (ii) For $P_{S,D} k_{\text{BIA}}$ and $E = 0$ the spin precession is suppressed because $P_{S,D} k_{\text{BIA}}$. In this case we have $\cos = 1$ independent of the channel length L . For $E > 0$ the spin states start to precess. Here spin precession and \cos are more complicated functions of E because E changes both the magnitude and orientation of B . (iii) For a QW grown in the high-symmetry crystallographic direction $[001]$ the overlap \cos is symmetric with respect to $E > 0$ and $E < 0$. In the latter case the roles of k_k $[110]$ and k_k $[110]$ are reversed.

It is interesting to compare Fig. 5 with the magnitude of spin splitting k as a function of electric field E (Fig. 6). We see that k depends rather sensitively on both the magnitude and orientation of the wave vector k_k . Nevertheless, we obtain in Fig. 5 the same modulation of the overlap \cos as a function of E for k_k $[110]$ and k_k $[110]$, independent of the magnitude of k_k [apart from a constant phase shift $\phi_0(k_k)$]. This is due to the fact that the relevant quantity for the spin transistor is not the absolute value k of the spin splitting, but the variation $\partial(k)/\partial E$. We see in Fig. 6 that the latter quantity depends much more weakly on the magnitude and orientation of k_k . Furthermore, it is advantageous

that the orientation of $B(k_k)$ is independent of the magnitude of the tunable part of the spin-orbit interaction. It can be seen in Fig. 3 that this condition is fulfilled for k_k $[110]$ and k_k $[110]$ but not for k_k $[100]$. Therefore the modulation of \cos as a function of E is more pronounced in the former case than for k_k $[100]$, even though in all cases the spin splitting k shows roughly the same field dependence $\partial(k)/\partial E$.

D. Spin Precession and Spin Relaxation

For the Datta spin transistor it is advantageous to have a small spin relaxation in the semiconducting channel because spin relaxation is competing with the controlled spin precession in the channel. Typically, the dominant mechanism for spin relaxation in 2D electron systems is the one proposed by D'yakonov and Perel' (DP).^{17,35} It can be viewed as a spin precession in the effective field B that is randomized because B changes when momentum scattering changes the wave vector k_k of the electrons. DP spin relaxation can therefore be suppressed if (apart from a sign of B) the orientation of B is independent of the wave vector k_k and the spins of the propagating electrons are oriented parallel to B . Such a situation can be realized in a symmetric QW grown in the crystallographic direction $[110]$ where B is perpendicular to the plane of the QW,^{35,36} see Fig. 3(e). Similarly, in a QW grown in the crystallographic direction $[001]$ with $j = j_w$ we have in first order of k_k that B $[110]$ (or B $[110]$) depending on the sign of α and β .²⁰ In both cases spin relaxation is suppressed only for a particular value of the Rashba spin-orbit coupling (i.e., a particular value of the field E). For the spin transistor it is preferable to have a regime of electric fields E with suppressed spin relaxation so that we can switch between $\cos = 1$ and $\cos = -1$.

Recently, an alternative spin transistor has been proposed²⁰ that is less sensitive to spin relaxation. It uses the fact that not only DP spin relaxation can be suppressed if (apart from a sign of B) the orientation of the effective field B is the same for all wave vectors k_k ; but obviously spin precession is then suppressed, too. Therefore, if B $k_{S,D}$ electrons travel unperturbed through the device which corresponds to the "on" state. In a detuned system, on the other hand, B varies as a function of k_k which implies that, in general, $B \neq P_{S,D}$. Therefore, spin precession and/or DP spin relaxation reorient the spins in the channel. The spin vector $\hbar s$ ($x = L$) is thus no longer matches the polarization P_D of the drain contact so that the current through the device diminishes.

Such a spin transistor can be built using a QW grown in the crystallographic direction $[110]$. Here it follows from Fig. 3(e) that if the QW is symmetric then DP spin relaxation is suppressed because B is perpendicular to the plane of the QW for all in-plane wave vectors k_k . If $P_{S,D} k_{\text{BIA}}$ electrons thus travel unperturbed through the device. If the QW is made asymmetric by applying an electric field E perpendicular to the plane of the well, the

current diminishes because of the onset of spin precession and/or DP spin relaxation.

Alternatively, we can use a QW grown in the crystallographic direction [001] (Ref. 20). Here we can achieve in linear order of k_k that B is independent of k_k if $j = j_z$. This situation is approximately shown by the innermost contour in Fig. 3(d). Note, however, that higher orders in spin splitting [in particular the cubic term in Eq. (16)] do not comply with the requirement that in the on state of the device the orientation of B should be independent of k_k . Furthermore, we see in Fig. 3(d) that only the orientation but not the magnitude of B is independent of k_k . For electrons with $k_k \parallel [110]$ we have actually $B = 0$ whereas B is the largest for $k_k \parallel [\bar{1}\bar{1}0]$. In the former case (i.e., for $P_{SD} \propto k_k \parallel [110]$) changing E diminishes the current through the device because we have then $P_{SD} \propto B$ so that injected electrons precess around B . The electrons do not precess in the latter case because we have $P_{SD} \propto B$ independent of E . DP spin relaxation is highly anisotropic, too. Here the situation is actually reversed: We have large spin relaxation rates for those directions of hSi for which we have a large $B(k_k)$ (Refs. 43,44). Therefore, spin relaxation supports the switching of the device most effectively if $k_k \parallel [\bar{1}\bar{1}0]$. We remark that an all-inclusive investigation of this question should explicitly evaluate spin relaxation as a function of k_k and hSi .

IV. CONCLUSIONS

In general, the total $B = 0$ spin splitting in inversion asymmetric 2D systems is determined by an interplay of spin splitting due to BIA, which is always present in systems with a zinc blende structure, and the tunable spin splitting due to SIA. These spin splittings can be characterized by effective magnetic fields $B(k_k)$ that vary as

a function of in-plane wave vector k_k . The functional form of $B_{SIA}(k_k)$ due to SIA is independent of the crystallographic direction in which a QW has been grown. Due to the axial symmetry of the Rashba term the $B_{SIA}(k_k)$ is always perpendicular to k_k in the plane of the QW. Furthermore, it is only weakly dependent on the magnitude of k_k . On the other hand, the field $B_{BIA}(k_k)$ due to BIA depends sensitively both on the magnitude and orientation of k_k as well as on the crystallographic direction in which the QW was grown. For QW's grown in the direction [001] the field $B_{BIA}(k_k)$ is always in the plane of the QW whereas for QW's grown in the direction [110] it is pointing perpendicular to the plane of the QW. For other growth directions the field $B_{BIA}(k_k)$ has both in-plane and out-of-plane components.

Electrons injected into a 2D semiconducting channel propagate with a certain in-plane wave vector k_k . If these electrons are spin-polarized such that the spinor $j_{\pm i}$ of the electrons is not a spin eigenstate of the system, the spin of the propagating electrons precesses in the effective field $B(k_k)$. The precession is the largest if the spin orientation hSi of the electrons is perpendicular to the effective field $B(k_k)$. In a QW grown in the crystallographic direction [001] it is thus advantageous that the electrons are injected in the in-plane directions $[1\bar{1}0]$ or $[110]$ because here the field $B(k_k)$ is always perpendicular to the direction of propagation. For the direction $[100]$, on the other hand, the fields due to BIA and SIA are perpendicular to each other so that the orientation of the total field $B(k_k)$ depends on the magnitude of BIA and SIA spin splitting.

Acknowledgments

The author would like to thank U. Merkt and G. Meier for stimulating discussions and suggestions.

- ¹ C. Kittel, *Quantum Theory of Solids* (Wiley, New York, 1963).
- ² G. Dresselhaus, *Phys. Rev.* **100**, 580 (1955).
- ³ Y. A. Bychkov and E. I. Rashba, *J. Phys. C: Solid State Phys.* **17**, 6039 (1984).
- ⁴ S. J. Papadakis, E. P. De Poortere, H. C. Manoharan, M. Shayegan, and R. Winkler, *Science* **283**, 2056 (1999).
- ⁵ M. I. Dyakonov and V. I. Perel, in *Optical Orientation*, edited by F. Meier and B. P. Zakharchenya (Elsevier, Amsterdam, 1984), vol. 8 of *Modern Problems in Condensed Matter Sciences*, chap. 2, pp. 11{71.
- ⁶ G. E. Pikus and A. N. Titkov, in *Optical Orientation*, edited by F. Meier and B. P. Zakharchenya (Elsevier, Amsterdam, 1984), vol. 8 of *Modern Problems in Condensed Matter Sciences*, chap. 3, pp. 73{131.
- ⁷ F. G. Pikus and G. E. Pikus, *Phys. Rev. B* **51**, 16928 (1995).
- ⁸ S. A. Wolf, D. D. Awschalom, R. A. Buhrman, J. M. Daughton, S. von Molnar, M. L. Roukes, A. Y. Chtchelkanova, and D. M. Treger, *Science* **294**, 1488 (2001).

- ⁹ E. A. de Andrada e Silva, *Phys. Rev. B* **46**, 1921 (1992).
- ¹⁰ F. M. Alcher, G. Lommer, and U. Rossler, *Superlatt. Microstruct.* **2**, 267 (1986).
- ¹¹ R. Eppenga and M. F. H. Schuurmans, *Phys. Rev. B* **37**, 10923 (1988).
- ¹² G. E. Pikus, V. A. Manushchak, and A. N. Titkov, *Sov. Phys. Semicond.* **22**, 115 (1988).
- ¹³ H.-R. Trebin, U. Rossler, and R. Ranvaud, *Phys. Rev. B* **20**, 686 (1979).
- ¹⁴ U. Rossler, *Solid State Commun.* **49**, 943 (1984).
- ¹⁵ L. W. Essinger, U. Rossler, R. Winkler, B. Jusserand, and D. Richards, *Phys. Rev. B* **58**, 15375 (1998).
- ¹⁶ R. Winkler and U. Rossler, *Phys. Rev. B* **48**, 8918 (1993).
- ¹⁷ M. I. Dyakonov and V. I. Perel, *Sov. Phys. (Solid State)* **13**, 3023 (1972).
- ¹⁸ S. Datta and B. Das, *Appl. Phys. Lett.* **56**, 665 (1990).
- ¹⁹ T. Matsuyama, C.-M. Hu, D. Grunler, G. Meier, and U. Merkt, *Phys. Rev. B* **65**, 155322 (2002).

- ²⁰ J. Schliemann, J. C. Egues, and D. Loss, Phys. Rev. Lett. 90, 146801 (2003).
- ²¹ T. Schapers, G. Engels, J. Lange, T. Klocke, M. Hollfelder, and H. Luth, J. Appl. Phys. 83, 4324 (1998).
- ²² P. R. Hammar and M. Johnson, Phys. Rev. B 61, 7207 (2000).
- ²³ H. Ohno, ed., Proceedings of the First International Conference on the Physics and Applications of Spin Related Phenomena in Semiconductors, vol. 10 of Physica E (2001).
- ²⁴ J. M. Luttinger, Phys. Rev. 102, 1030 (1956).
- ²⁵ M. Altarelli, J. Lum. 30, 472 (1985).
- ²⁶ J. Luo, H. Munekata, F. F. Fang, and P. J. Stiles, Phys. Rev. B 38, 10142 (1988).
- ²⁷ B. Das, D. C. Miller, S. Datta, R. Reifengerger, W. P. Hong, P. K. Bhattacharya, J. Singh, and M. Jaffe, Phys. Rev. B 39, 1411 (1989).
- ²⁸ G. Engels, J. Lange, T. Schapers, and H. Luth, Phys. Rev. B 55, R1958 (1997).
- ²⁹ D. Grundler, Phys. Rev. Lett. 84, 6074 (2000).
- ³⁰ R. Winkler, S. J. Papadakis, E. P. De Poortere, and M. Shayegan, Phys. Rev. Lett. 84, 713 (2000).
- ³¹ S. Keppler and R. Winkler, Phys. Rev. Lett. 88, 046401 (2002).
- ³² From a group theoretical point of view this can be traced back to the fact that $j + (k_k)i$ and $j - (k_k)i$ transform according to different irreducible representations of the group of the wave vector k_k .
- ³³ G. L. Bir and G. E. Pikus, Symmetry and Strain-Induced Effects in Semiconductors (Wiley, New York, 1974).
- ³⁴ For a symmetric QW grown in the crystallographic direction [110] the symmetry axis of the point group C_{2v} is parallel to the axis [001] in the plane of the QW.
- ³⁵ M. I. Dyakonov and V. Y. Kachorovski, Sov. Phys. Semicond. 20, 110 (1986).
- ³⁶ Y. Ohno, R. Terauchi, T. Adachi, F. Matsukura, and H. Ohno, Phys. Rev. Lett. 83, 4196 (1999).
- ³⁷ R. H. Park, Phys. Rev. 100, 573 (1955).
- ³⁸ J. Nitta, T. Akazaki, H. Takayanagi, and T. Enoki, Phys. Rev. Lett. 78, 1335 (1997).
- ³⁹ J. J. Sakurai, Modern Quantum Mechanics (Addison-Wesley, Redwood City, 1994), revised ed.
- ⁴⁰ G. Schmidt, D. Ferrand, L. W. Molenkamp, A. T. Filip, and B. J. van Wees, Phys. Rev. B 62, 4790 (2000).
- ⁴¹ E. I. Rashba, Phys. Rev. B 62, 16267 (2000).
- ⁴² A. Fert and H. Jares, Phys. Rev. B 64, 184420 (2001).
- ⁴³ N. S. Averkiev and L. E. Glub, Phys. Rev. B 60, 15582 (1999).
- ⁴⁴ J. Kainz, U. Rossler, and R. Winkler, cond-mat/0304017.